Identity of InSb-II and InSb-III

R. J. Nelmes and M. I. McMahon

Department of Physics and Astronomy, The University of Edinburgh,
Mayfield Road, Edinburgh, EH9 3JZ, United Kingdom
(Received 18 March 1996)

The well-known phase transition from InSb-IV to InSb-III at ~10 GPa has been studied using angle-dispersive powder-diffraction techniques. It is shown that the transition proceeds through a previously undetected intermediate phase, and that InSb-III is in fact identical with InSb-II. The apparently well-established *P-T* phase diagram is thus substantially incorrect. [S0031-9007(96)00622-9]

PACS numbers: 61.50.Ks, 61.10.Nz, 62.50.+p

InSb is one of the most extensively studied of all the III-V semiconductors. A phase transition under pressure was first reported in 1960 [1], and by the end of that decade the complete *P-T* phase diagram shown in Fig. 1 had been mapped out [2,3]. The ambient-pressure phase I has the zinc-blende structure; phase II was found to have the diatomic equivalent of the β-tin structure; a simple orthorhombic (*Pmm*2) structure was reported for phase IV, with atoms at $(0,0,0)$ and $(0,1/2,\alpha \sim 1/2)$ [4]; and phase III was indexed on a hexagonal unit cell [3]. A decade later, with improved experimental techniques, Yu, Spain, and Skelton [5] showed that a better fit to the phase III powder pattern at 11.5 GPa was obtained with a primitive orthorhombic unit cell, twice the volume of that of phase IV; they confirmed the reported structure for phase IV, apart from adjusting the value of α to $\sim 1/4$. In the first synchrotron source study, Vanderborgh, Vohra, and Ruoff [6] reported a new phase V, appearing at 6.3 GPa, and then a gradual transition to (hexagonal) phase III completed at 17.5 GPa, a much higher pressure than previously reported. Apart from these last results, the phase diagram in Fig. 1 has appeared to be confirmed by many studies, and has remained widely accepted [7], except for some uncertainty as to whether the structure of phase III is orthorhombic or hexagonal.

In a recent detailed study of InSb to 5 GPa, we showed that the low-pressure part of the phase diagram is certainly incorrect [8]. Two different behaviors are found when the zinc-blende phase is compressed. Either (i) there is a transition at ~2.1 GPa to a mixture of a site-disordered β-tin-like phase (*P2*) and an orthorhombic phase (*P3*), which then recrystallizes over a period of several hours to a different orthorhombic phase (*P4*), or (ii) there is a superpressed transition directly to *P4* at ~3 GPa. *P4* is the equilibrium phase in the pressure range from 2 GPa to at least 5 GPa, and can be identified as InSb-IV. However, the true structure is much more complex than previously supposed; it is a site-ordered superstructure in which the previously reported unit cell is an average subcell [9]. *P3* can be identified as InSb-II, but does *not* have the β-tin structure. It is clearly body-centered *orthorhombic,* and is site ordered, with In at $(0,0,0)$ and Sb at $(0,1/2,\delta \sim 1/2)$. If $\delta = 1/2$ the

space group is *Immm*, and otherwise it is *Imm*2; measured intensities indicate that it is *Immm*. Importantly, we could find no pressure (in the range up to ~5 GPa) at which *P3* (InSb-II) is the stable phase [8]. However, the rate of recrystallization to *P4* is reduced by increasing pressure, and the transformation effectively ceases above ~3 GPa. Indeed, a sample of *P3* taken above ~3 GPa within an hour or so of formation remains in the *P3* phase indefinitely. The inhibition of the *P3* to *P4* transition with increasing pressure is to be expected since *P4* is ~0.5% *less* dense than *P3*. Probably for the same reason, recrystallization does not proceed beyond a ~50:50 mixture of *P3* and *P4* even below 3 GPa. However, complete recrystallization to *P4* is achieved at modest temperatures of ~50–100 °C. Powder patterns from InSb at room temperature thus commonly have approximately equal amounts of *P3* and *P4*, with a small but clearly detectable residue of *P2* (which has almost the same density as *P3*, and does not quite completely transform to *P3* at room temperature [8]). The supposed new phase V of Vanderborgh *et al.* [6] can be accounted for entirely by such a mixture of these three phases.

Thus, not only are the structures previously found for InSb-II and InSb-IV incorrect, but so are their fields of stability in Fig. 1. As summarized in Ref. [8], much of the original evidence for the phase diagram was obtained by quenching to ~80 K and then releasing the pressure to
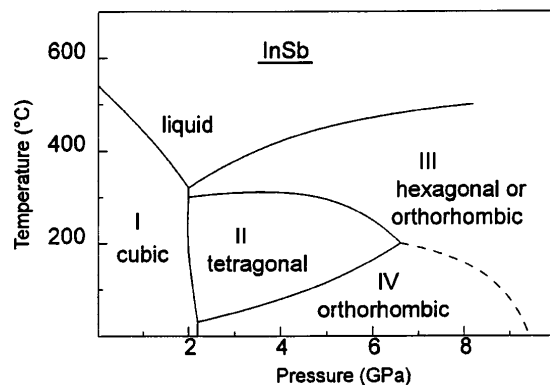

FIG. 1. Previously accepted phase diagram of InSb, after Refs. [3] and [5].

study the recovered phase, which is stable if kept below 210 K. This phase has a β-tin-like structure, and was wrongly believed to be identical with InSb-II. What seems probable is that the recovered phase is the same as the new phase $P2$.

In this Letter we now report an investigation of the transition to phase III, and the nature of its structure. Remarkably, *we find that phase III is one and the same as phase II.* Both are $P3$. We show that $P4$ transforms to $P3$ above ~10 GPa, through a new, intermediate phase that we label $P5$. At ~17 GPa, $P3$ starts to transform to another intermediate phase and then to the bcc phase at ~21 GPa—well below the previously reported transition pressure of 28 GPa [6]. $P3$ transforms back to $P4$ at ~4 GPa on pressure decrease. The stability domain of $P3$ (InSb-II) at room temperature is thus from ~7 to ~17 GPa, and the separate occurrence of $P3$ at 2–3 GPa—as an intermediate stage in the $P1 \rightarrow P4$ transition—remains to be explained. What emerges is that one of the apparently best known and carefully determined of all the semiconductor phase diagrams is substantially incorrect.

Finely ground, 99.9999% InSb—from the same source as for our previous studies [8]—was loaded into Merrill-Bassett and Diacell [10] diamond-anvil pressure cells with a 4:1 mixture of methanol:ethanol as a pressure transmitting medium, and chips of ruby to allow the sample pressure to be measured by the ruby fluorescence technique [11]. Some samples were converted into the $P3$ phase (with, as always, a residue of $P2$), and taken quickly

above ~3 GPa to prevent any transformation to $P4$. Other samples were converted to single-phase $P4$ by compression at ~100 °C. X-ray diffraction data were collected at room temperature on station 9.1 at SRS, Daresbury, using angle-dispersive techniques and an image-plate area detector, with an incident wavelength of 0.4447 Å. The details of the beam-line setup, experimental procedures, and data analysis are as previously published [12]. Lattice parameters were obtained by profile fitting using MPROF [13] for single-phase patterns, and least-squares fits to measured d spacings for mixed-phase patterns.

On compression to ~15 GPa, the $P3$ diffraction pattern was found to remain unchanged apart from reduction in the unit-cell dimensions and some very small changes in axial ratios ($<1\%$). By contrast, the $P4$ phase shows some marked changes under increasing pressure. At ~5 GPa, the superstructure of $P4$ is made up of 6 NaCl-like layers stacked along y [14], with alternate layers displaced $\Delta \sim 0.2$ along z. (The y and z axes of Ref. [9] have been interchanged [14].) All the strong reflections in the diffraction pattern can be indexed to a simple, average $Pmm2$ subcell of dimensions $a_s = a/2$, $b_s = b/3$, and $c_s = c/2$, with sites at $(0,0,0)$ and $(0, 1/2, 2\Delta \sim 0.4)$. There are some relatively weak subcell reflections that would disappear if 2Δ approached 0.5, and thus made the subcell A-centered. These reflections are characteristic of $P4$ and remain clearly visible at ~8 GPa, as marked by asterisks in Fig. 2(a). (A few very weak superlattice reflections can also be seen, as marked by Δ symbols.) But on increasing pressure to
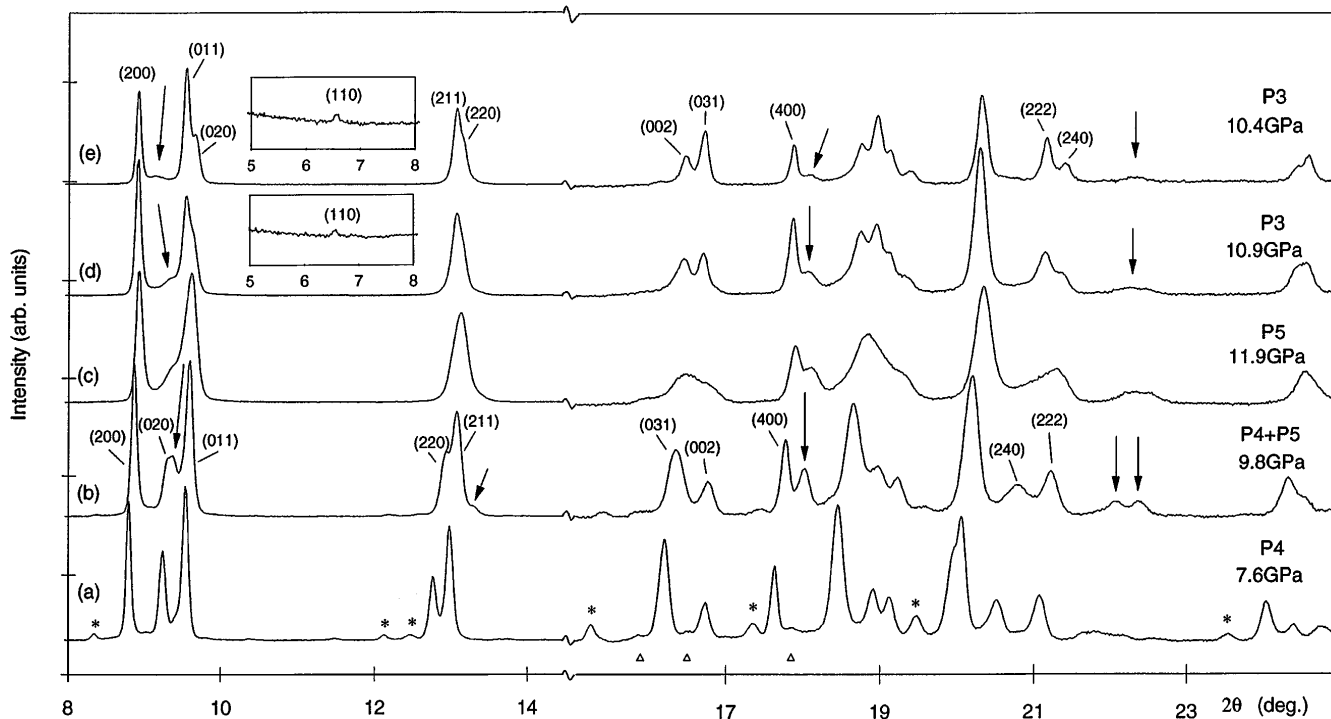

FIG. 2. Diffraction patterns from one sample of InSb in (a) phase $P4$, (b) phases $P4$ and $P5$ (arrowed), (c) phase $P5$, (d) phase $P3$ with residual $P5$ (arrowed), and (e) from another sample in phase $P3$ with residual $P2$ (arrowed). Above the break between $2\theta = 14°$ and $2\theta = 15°$, the intensity scale has been expanded to make the higher-angle peaks more clearly visible. Other details are described and discussed in the text. Insets show the very weak low-angle (110) reflection from profiles (d) and (e).

~10 GPa, all these reflections reduce strongly in intensity, and some new reflections emerge as marked by arrows in Fig. 2(b). The latter reflections reveal a transition to a new phase $P5$. We have found all $P4$ samples to go through this initial sequence of changes close to 10 GPa. However, the subsequent behavior varies.

A typical subsequent behavior is illustrated in Figs. 2(c) and 2(d), recorded 33 h apart. After a small further increase in pressure, the $P4$ phase transforms completely to $P5$, as shown in Fig. 2(c) by the complete disappearance of the reflections marked (*) in Fig. 2(a); and the $P5$ pattern broadens. Then, with time, a sharper and *different* pattern develops, as shown in Fig. 2(d). (This pattern also contains residual $P5$ peaks, as marked by arrows.) Figure 2(e) shows a pattern recorded from one of the samples initially formed as $P3$, including some weak residual $P2$ peaks, as marked by arrows. It can be seen that the non-$P5$ peaks in Fig. 2(d) agree closely with the $P3$ pattern, apart from some relatively small intensity differences that can be attributed to preferred orientation. A refinement of the $P3$ pattern in Fig. 2(e) gives cell dimensions of $a = 5.726(1)$ Å, $b = 5.279(1)$ Å, and $c = 3.104(1)$ Å and the indices of the strong lines on this cell are shown. The $P4$ pattern in the $P4/P5$ mixture of Fig. 2(b) can be refined on a corresponding $P4$ subcell with dimensions $2a_s = 5.769(2)$ Å, $b_s = 5.429(2)$ Å, and $c_s = 3.031(2)$ Å; and the strong lines are indexed on this cell in Fig. 2(b). The patterns in (b) and (e) are very similar in their strong lines apart from the quite large difference between b of $P3$ and b_s of $P4$. This difference is evident in the positions of the (020) reflections relative to (011), and the (220) reflections relative to (211) in the two profiles—and, at higher angles, (031) relative to (002), (240) relative to (222), and the resolution of the triplet at $2\theta \sim 19°$ in (b) into four distinct reflections in (e). All these distinguishing features of $P3$ can be seen in Fig. 2(d), except that the relative broadness of the $P3$ peaks in this figure obscures the (220) shoulder evident in Fig. 2(e). The non-$P5$ peaks in Fig. 2(d) fit very well to a $P3$ unit cell, with dimensions $a = 5.729(1)$ Å, $b = 5.286(2)$ Å, and $c = 3.105(1)$ Å. The weak (110) reflection of $P3$ in the inset of Fig. 2(e) arises from the small difference in scattering between In and Sb; detection of this reflection shows the structure to be site ordered. The clearly visible (110) reflection in the inset of Fig. 2(d) confirms that $P3$ formed from $P4$ is also site ordered.

The $P3$ and $P4$ unit cells are both close to meeting the condition for a hexagonal lattice, that the (011) and (020) peaks coincide (or $b = \sqrt{3}\,c$). Evidently, b/c is greater than $\sqrt{3}$ for $P4$ and less than $\sqrt{3}$ for $P3$, and this key difference between the two structures can be used to show the pressure dependence of their structural relationship, as in Fig. 3—which also includes points for the $P5$ phase. $P5$ patterns fit well to a site-disordered orthorhombic distortion of β-tin, with *Imma* symmetry—as found recently in GaSb [15]. The $P5$ unit cell is very similar to the $2a_s \times b_s \times c_s$ subcell of $P4$, but
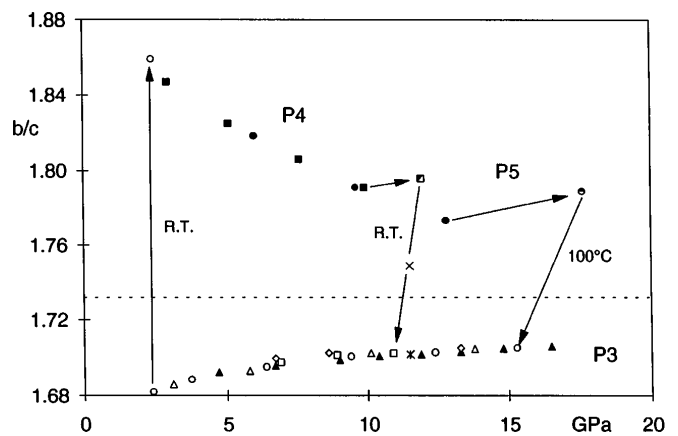

FIG. 3. Axial ratio b/c as a function of pressure in phases $P4$, $P5$, and $P3$ of InSb. Details, including the symbols, are described and discussed in the text. The dashed line shows the value of b/c required for a hexagonal lattice. RT denotes "room temperature."

with a slightly larger value for the b cell dimension. The filled symbols in Fig. 3 show the variation in b/c obtained for three samples initially made as $P3$ (filled triangles) and $P4$ (filled squares and circles) and taken up in pressure. Open symbols show values obtained on pressure decrease—as for the $P3$ sample (open triangle), which follows closely the curve obtained on pressure increase. The square symbols denote the sample whose patterns are shown in Figs 2(a) to 2(d): it transforms to $P5$ (half-filled square) and then—as shown by the arrows—to $P3$ (open square) at ~11 GPa. This $P3$ sample was taken down in pressure, and its b/c values clearly lie on the curve established by the sample initially made as $P3$ (solid and open triangles).

Different behavior was found in other samples left for similarly extended times in the $P4 + P5$ mixture of Fig. 2(c). Some made only a partial transformation to $P3$, and some transformed to a more broadened $P3$ pattern than that shown in Fig. 2(d). Sometimes single-phase $P5$ was as sharp as in the $P4 + P5$ mixture [unlike Fig. 2(c)]. In cases where the pressure was increased further on the $P4 + P5$ mixture or single-phase $P5$ before waiting for the transition to $P3$, the formation of $P3$ appeared to be inhibited. However, in all these cases, a complete transition to a sharp $P3$ pattern could be achieved by heating the sample to ~100 °C for about an hour. The $P4$ sample shown as a filled circle in Fig. 3 gives an example of this behavior. The pressure was increased quickly enough that the sample still had a significant $P4$ component at 13 GPa, and was not single-phase $P5$ (half-filled circle) until ~17 GPa. The transition to $P3$ (open circle) at ~15 GPa was then effected by heating at ~100 °C. This sample was also studied on pressure decrease (open circle), and eventually recrystallized back to $P4$ (open circle) at ~2.5 GPa—as shown by the arrow in Fig. 3.

It is clear that the transformation of $P4$ to $P3$ is quite complex; it occurs in two stages, first $P4$ to $P5$ and

665

then $P5$ to $P3$. The transition from $P4$ to $P5$ starts at 9.3(5) GPa in *all* samples, but—as shown—the transition from $P5$ to $P3$ can occur over a range of pressures (up to ~17 GPa), or not occur at all at room temperature. However, the evidence from samples left for many hours (or heated) at pressures just above 10 GPa is that $P3$ is the stable phase at room temperature (and up to at least 100 °C) above 10 GPa. All samples start to transform to another intermediate phase at ~17 GPa, and then to the bcc phase at 21(1) GPa (previously reported at 28 GPa [6]); and the bcc phase reverts directly to $P3$ at 20(1) GPa on pressure decrease. [Some points obtained from a $P3$ sample on pressure decrease from the bcc phase are included (open diamonds) in Fig. 3.] The $P3$ phase recrystallizes back to $P4$ at pressures varying from 4 GPa down to 2.5 GPa. $P3$ may thus be the equilibrium stable phase from as low as ~7 GPa, but this is uncertain until the stability range of $P5$ is established.

Our principal conclusions are thus that the transition from InSb-IV to InSb-III proceeds through a previously undetected intermediate phase, and that InSb-III is, in fact, the same orthorhombic phase as InSb-II ($P3$ in our labeling). It is rewarding to look back to earlier work with this perspective. A full 30 years ago, Martin and Smith [16] reported that the "β-tin phase" (almost certainly $P3$) compressed unchanged to ~26 GPa where two additional lines were detected that could be interpreted as a transition to a bcc phase. This is exactly what we now observe for a sample made initially as $P3$, except that we detect the transition to bcc at a lower pressure. The much later, higher-quality data of Yu *et al.* [5] showed a clear change in the $P4$ pattern starting at 9 GPa (as we find), and revealed that the new phase was described better as orthorhombic rather than hexagonal (as previously proposed) at 11.5 GPa. However, they found a *primitive* cell. In fact, their observed d spacings (their Table III) can be indexed to a $P3$ cell with body-centering absences, with $a = 5.710(4)$ Å, $b = 5.271(4)$ Å, and $c = 3.097(2)$ Å; and this cell fits their d_{obs} values with an average discrepancy some three times smaller than is given by their proposed cell. The point labeled $\times$ in Fig. 3 shows b/c for their cell, and the symbol $*$ marks the value obtained from their data with the $P3$ indexing. The latter value falls on the curve of our $P3$ results remarkably well. In the recent study by Vanderborgh *et al.* [6] there is evidence—as we have previously discussed [8]—that their samples were $P3/P4$ mixtures. They reported a gradually improving fit to a hexagonal unit cell, completed at ~17.5 GPa. At this pressure, according to our results, their samples would have been either pure $P3$ or a $P3/P5$ mixture, which would both give diffraction patterns close to hexagonal in appearance (see Figs. 2 and 3). In fact, the pattern shown for InSb at 17.5 GPa in their Fig. 2 corresponds closely to a lower resolution pattern from $P3$ in terms of the relative peak widths—there is, perhaps, even a discernible shoulder on their "(101)" reflection corresponding to the (211)/(220) doublet of $P3$.

It is clear now that the derivation of the InSb phase diagram became misdirected by two main factors—first, the erroneous conviction that InSb-II and the phase recovered to ambient pressure at low temperature were the same (as discussed in Ref. [8]), and, second, the curious "precursor" appearance of InSb-II ($P3$) at pressures well below its apparent equilibrium field. As a result, studies of InSb have long been influenced by a substantially incorrect phase diagram. With this recognized, there remains much of interest yet to be understood about this fascinating system, including the subtle interplay between the $P3$ and $P4$ phases, the complex transition mechanisms apparently involving the intermediate $P2$ and $P5$ phases, and, of course, the mapping out of the true P-T phase diagram.

[1] H. A. Gebbie, P. L. Smith, I. G. Austin, and J. H. King, Nature (London) **188**, 1096 (1960).
[2] M. D. Banus and M. C. Lavine, J. Appl. Phys. **38**, 2042 (1967).
[3] M. D. Banus and M. C. Lavine, J. Appl. Phys. **40**, 409 (1969).
[4] J. S. Kasper and H. Brandhorst, J. Chem. Phys. **41**, 3768 (1964).
[5] S. C. Yu, I. L. Spain, and E. F. Skelton, J. Appl. Phys. **49**, 4741 (1978).
[6] C. A. Vanderborgh, Y. K. Vohra, and A. L. Ruoff, Phys. Rev. B **40**, 12 450 (1989).
[7] E. Yu. Tonkov, *High Pressure Phase Transformations* (OPA, Amsterdam, 1992), Vol. II, p. 503.
[8] R. J. Nelmes, M. I. McMahon, P. D. Hatton, J. Crain, and R. O. Piltz, Phys. Rev. B **47**, 35 (1993).
[9] R. J. Nelmes and M. I. McMahon, Phys. Rev. Lett. **74**, 106 (1995).
[10] D. M. Adams, Diacell Products, 54 Ash Tree Road, Leicester, UK.
[11] H. K. Mao and P. M. Bell, Science **200**, 1145 (1978).
[12] R. J. Nelmes and M. I. McMahon, J. Synchrotron Radiat. **1**, 69 (1994).
[13] A. N. Fitch and A. D. Murray (unpublished).
[14] For the standard setting of the $P4$ structure in space group *Cmcm*, the NaCl-like layers are stacked along the z axis (see Ref. [9]). However, for ease of comparison with the lattice parameters of $P3$, it is convenient to interchange the y and z axes. [This *B*-face centered setting was also the one adopted in the initial report of the $P4$ phase in Ref. [8].]
[15] M. I. McMahon, R. J. Nelmes, N. G. Wright, and D. R. Allan, Phys. Rev. B **50**, 13 047 (1994).
[16] J. E. Martin and P. L. Smith, Brit. J. Appl. Phys. **16**, 495 (1965).